DALTON
FULL PAPER

Coordination networks of Ag(I) and *N,N′*- bis(3-pyridinecarboxamide)-1,6-hexane: structures and anion exchange

Sebastian Muthu, John H. K. Yip* and Jagadese J. Vittal

Department of Chemistry, The National University of Singapore, 10 Kent Ridge Crescent, 119269, Singapore

Received 9th July 2002, Accepted 3rd October 2002
First published as an Advance Article on the web 6th November 2002

A bidentate ligand *N,N′*- bis(3-pyridinecarboxamide)-1,6-hexane (L) and its silver complexes have been synthesized and characterized by single crystal X-ray diffraction. Reaction of $AgClO_4$ and L in H_2O/EtOH gives rise to a coordination polymer $[Ag_2L_3OH][ClO_4]\cdot 2.5H_2O$. The X-ray crystal structure of the compound shows honeycomb-like networks in which four-coordinated Ag ions are linked to three-coordinated Ag ions *via* three ligands L. The coordination of the long ligands L to the Ag ions creates tube-like structures and the tubes of adjacent honeycomb layers are interlocked, leading to an interpenetrating network. The compound $[AgL][ClO_4]$, synthesized from CH_3OH, is composed of twisted zigzag coordination polymers in which ligands L are linked by Ag ions. Ligand L displays two different conformations **A** and **B** within a single strain of polymer. The two conformers differ in the orientation of the two pyridyl-groups which are arranged periodically in the polymer in the sequence **ABBABBA**. The polymer chains assemble into 2-D undulating sheets *via* amide hydrogen bonds. Reaction between $AgNO_3$/$AgCF_3SO_3$ and L leads to polymeric compounds $[AgL][NO_3]$ and $[AgL][CF_3SO_3]$. The compounds are composed of coordination polymers in zigzag conformation and the polymer chains assemble into undulating sheets *via* inter-chain hydrogen bonds. The inter-sheet Ag–Ag distances of the compounds are in the order $[AgL][CF_3SO_3] > [AgL][ClO_4] > [AgL][NO_3]$. The anion exchange properties of the compounds are monitored by using X-ray powder diffraction, infrared spectroscopy and elemental analysis. Our results show that the anions in $[AgL][NO_3]$ and $[AgL][CF_3SO_3]$ can be totally replaced with ClO_4^-. However, the exchange is not reversible. In additional, inter-conversion between $[AgL][NO_3]$ and $[AgL][CF_3SO_3]$ by anion exchange is shown to be unfeasible. Anion selectivity could be due to the different hydration energy of the anions and the structural reorganization involved in the conversion.

Introduction

The synthesis of coordination polymers is a rapidly expanding field of research.[1] Given the high directionality of metal–ligand bonds and the regular geometry of metal complexes, it is possible to control the 3-D structures of coordination polymers by judicial choice of metal ion and design of ligand and based on this synthetic strategy, numerous intriguing 2-D and 3-D polymeric structures have been created.[1–4] Aside from their interesting structures, coordination polymers are attractive because of their modular nature which makes incorporation of functional groups into a 3-D network synthetically straightforward. This allows a bottom-up approach to functional materials.[5] There are examples showing that coordination polymer networks can be applied to anion exchange,[6] chemical sensing[7] and gas storage.[8] Our recent study[9] showed that the compound *N,N′*- bis(3-pyridinecarboxamide)-1,2-ethane, similar to many other bipyridines, is capable of forming coordination polymers with d^{10} Ag^I, Zn^{II} and Cd^{II} ions. A special feature of the Ag(I) polymers is that the polymer chains can zip up into 2-D undulating sheets *via* inter-chain amide hydrogen bonds. The possibility that increasing the length of the bridging ligand would form flexible coordination frameworks of high porosity or coordination polymers with interesting interpenetration[10] have led us to study the ligand *N,N′*-bis-(3-pyridinecarboxamide)-1,6-hexane (L) (Scheme 1). Unlike *N,N′*-bis(3-pyridinecarboxamide)-1,2-ethane, the ligand L is found to form 3-D hexagonal nets with Ag(I) ions. In addition, we also showed that Ag and L form zigzag coordination polymers [AgL][X] ($X = ClO_4^-$, NO_3^- or $CF_3SO_3^-$) whose structures were characterized by single crystal X-ray diffraction. Recently, the anion exchange behavior of some coordination polymers has been examined and the results highlighted the potential applications of the polymers to anion sequestering[6] and sensing.[7] To explore the properties of the coordination polymers, the anion exchange reactions of the three [AgL][X] compounds were investigated by using X-ray powder diffraction, infrared absorption spectroscopy and elemental analysis.

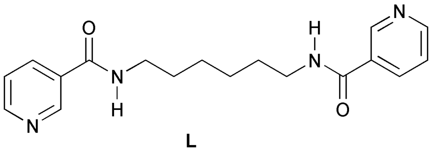

Scheme 1

Experimental

General methods

All chemicals were purchased from Aldrich and used without further purification. ^1H-NMR and IR spectra (KBr pellet) spectra were recorded on a Bruker ACF 300 spectrometer and a Bio-Rad FTIR spectrometer, respectively. Electrospray mass spectra (ES-MS) were measured on a Finnigan-MAT 731 spectrometer with HPLC-grade MeOH as mobile phase. Elemental analyses were carried out in the microanlytical laboratory in the Department of Chemistry, The National University of Singapore.

DOI: 10.1039/b206680g

Synthesis

***N,N′*-Bis(3-pyridinecarboxamide)-1,6-hexane (L).** 1,6-Hexanediamine (1 g, 17 mmol) was slowly added to a pyridine solution (50 ml) of 3-pyridnecarboxylic acid (4.23 g,34 mmol). The mixture was stirred for 15 min and triphenyl phosphite (9 ml, 34 mmol) was added slowly through a dropping funnel over the period of 15 min. The mixture was refluxed for 6 h and then the volume was reduced to 10 ml by vacuum evaporation. A white precipitate was obtained from the solution after standing at room temperature for 24 h. The solid was filtered off and washed with cold water. Recrystallization from ethanol gave colorless crystals. Yield 70%. ^{1}H NMR ($CDCl_3$, δ) 9.03 (2H, s, H2-py), 8.7 (2H, d, H4-py), 8.14 (2H, d, H6-py), 7.35 (2H, t, 5H-py), 6.7 (2H, s, NH), 3.46 (4H, t, N–C*H*$_2$), 1.64 (4H, p, N–CH$_2$–C*H*$_2$), 1.44 (4H, p, N–CH$_2$–CH$_2$–C*H*$_2$), mp: 169–172 °C. Anal Calcd(%) for $C_{18}H_{22}N_4O_2$: C, 66.26; H, 6.74; N, 17.18. Found(%): C, 66.02; H, 6.41; N, 16.83. ES-MS: M$^+$, 326; [M + H]$^+$, 327.

[Ag$_2$L$_3$OH][ClO$_4$]·2.5H$_2$O. An ethanol solution of L (0.33 g, 1 mmol) was layered on top of an aqueous solution of $AgClO_4$ (0.21 g, 1 mmol). After three weeks, large cubic crystals of the compound were found at the interface. Yield 20%. Anal Calcd(%) for $C_{54}H_{72}N_{12}O_{13.5}ClAg_2$: C, 47.81; H, 5.31; N, 12.39. Found(%): C, 47.15; H, 5.26; N, 12.41. IR (cm^{-1}), $\nu(ClO_4)$, 1145 (s).

[AgL][ClO$_4$]. L (0.33 g, 1 mmol) was dissolved in 20 ml of methanol and $AgClO_4$ (0.20 g, 1 mmol) was added and stirred for 1 h. The white precipitate obtained was filtered off and washed with an excess of methanol. Needle like crystals were obtained by slow diffusion of diethyl ether into a CH_3CN solution of the compound.. Yield 70%. ^{1}H NMR (CD_3CN, δ) 8.91 (2H, s, H2-py), 8.63 (2H, d, H4-py), 8.11 (2H, d, H6-py), 7.44 (2H, t, 5H-py), 7.12 (2H, s, NH), 3.33 (4H, t, N–C*H*$_2$), 1.58 (4H, p, N–CH$_2$–C*H*$_2$), 1.42 (4H, p, N–CH$_2$–CH$_2$–C*H*$_2$). Anal Calcd(%) for $C_{18}H_{22}N_4O_6ClAg$: C, 40.49; H, 6.74; N, 10.50. Found(%): C, 40.63; H, 4.14; N, 10.61. IR (cm^{-1}), $\nu(ClO_4)$, 1145 (s). ES-MS: M$^+$, 433.4; [M + 2]$^+$, 435.4.

[AgL][NO$_3$]. 0.17 g of $AgNO_3$ (1 mmol) was added to a methanol solution of L (0.33 g, 1 mmol). A white precipitate appeared immediately and the mixture was stirred for 1 h at room temperature. The white solid collected after filtration was washed with an excess of methanol. Colorless crystals were obtained by slow evaporation of a CH_3CN solution of the compound. Yield 65%. ^{1}H NMR (CD_3CN, δ) 8.93 (2H, s, H2-py), 8.65 (2H, d, H4-py), 8.07 (2H, d, H6-py), 7.4 (2H, t, 5H-py), 7.14 (2H, s, NH), 3.35 (4H, t, N–C*H*$_2$), 1.58 (4H, p, N–CH$_2$–C*H*$_2$), 1.42 (4H, p, N–CH$_2$–CH$_2$–C*H*$_2$). Anal Calcd(%) for $C_{18}H_{22}N_5O_5Ag$: C, 43.56; H, 4.44; N, 14.11. Found(%): C, 43.44; H, 4.62; N, 13.91. IR (cm^{-1}), $\nu(NO_3)$, 1384 (s). ES-MS: M$^+$, 433.4; [M + 2]$^+$, 435.

[AgL][CF$_3$SO$_3$]. The compound was synthesized by layering an ethanol solution of L (0.33 g, 1 mmol) over an aqueous solution of $AgCF_3SO_3$(0.25 g, 1 mmol). Slow diffusion of the solutions led to the formation of cubic crystals. Yield 45%. ^{1}H NMR (CD_3CN, δ) 8.92 (2H, s, H2-py), 8.64 (2H, d, H4-py), 8.08 (2H, d, H6-py), 7.43 (2H, t, 5H-py), 7.16 (2H, s, NH), 3.35 (4H, t, N–C*H*$_2$), 1.50 (4H, p, N–CH$_2$–C*H*$_2$), 1.40 (4H, p, N–CH$_2$–CH$_2$–C*H*$_2$). Anal Calcd(%) for $C_{19}H_{22}F_3N_4O_5SAg$: C, 39.11; H, 3.77; N, 9.61. Found(%): C, 39.21; H, 3.56; N, 9.55. IR (cm^{-1}), $\nu(CF_3SO_3)$, 1261 (s). ES-MS: M$^+$, 433.4; [M + 2]$^+$, 435.4.

Anion exchange

In a typical anion exchange experiment, crystals of [AgL][X] (X = NO_3, ClO_4, CF_3SO_3) were suspended in a 10^{-2} M aqueous solution containing a different anion ($LiClO_4$, $LiCF_3SO_3$ or $NaNO_3$). The mixture was kept dark and stirred at room temperature for 12 h before filtration. Prolonged immersion (2 weeks) and higher salt concentrations (0.1 M) were used for the exchange reactions $[AgL][ClO_4] + NO_3^-/CF_3SO_3^-$ and $[AgL][NO_3] + CF_3SO_3^- \leftrightarrow [AgL][CF_3SO_3] + NO_3^-$. The solids collected by filtration were washed extensively with water before being characterized by infrared spectroscopy, ESI mass spectrometry (negative mode), elemental analyses and X-ray powder diffraction.

X-Ray powder diffraction

X-Ray powder diffraction (XRPD) data were collected on a D5005 Bruker AXS X-ray diffractometer at 25 °C at 50 kV and 100 mA for Cu-α at a scan rate of 5° min^{-1}. The 2θ was increased at intervals of 0.02°. All the XRPD analyses were performed using a V12 sample holder.

X-Ray crystallography

The X-ray diffraction experiments were carried out on a Bruker SMART CCD diffractometer with a Mo-Kα sealed tube at 223(2) K. The wavelength of the radiation was 0.71073 Å. The program SMART[11] was used for collecting frames of data, SAINT[11] for integration of the intensity of reflections and scaling, SADABS[12] for absorption correction and SHELXTL[13] for space group and structure determination and least-square refinements on F^2. Anisotropic thermal parameters were refined for the non-hydrogen atoms. The hydrogen atoms were placed in ideal positions. The relevant crystallographic data and refinement details are shown in Table 1. The oxygen atoms of the perchlorate ion in [AgL][ClO$_4$] are disordered and are modeled with an occupancy of 0.5. Oxygen atoms O_3, O_4, O_{3A}, O_{4A} of $NO_3{}^-$ in [AgL][NO$_3$] are disordered and modeled with occupancies of 0.4 and 0.1. N_3 and O_3 are disordered with an occupancy of 0.5. Common isotropic thermal parameters were refined for the model. Soft constraints were applied for N–O, O–O distances using SADI.[13]

CCDC reference numbers 189551–189555.

See http://www.rsc.org/suppdata/dt/b2/b206680g/ for crystallographic data in CIF or other electronic format.

Results and discussion

N,N′-Bis(3-pyridinecarboxamide)-1,6-hexane (L)

The compound was synthesized by a condensation reaction between 3-pyridinecarboxylic acid and 0.5 mol of 1,6-hexanediamine. The compound is highly soluble in protic solvents such as water but insoluble in most of the organic solvents except dimethyl sulfoxide. The poor solubility is a sign of the presence of intermolecular hydrogen bonds. Indeed the X-ray crystal structure of the compound shows that molecules of L are aligned in parallel with the amide carbonyl of one chain directed toward the amide nitrogen of its two adjacent molecules (Fig. 1 and Table 2) and the N(H) ··· O=C distance of 2.990(2) Å compares favorably with the ones observed in amide hydrogen bonds.[14] Clearly the polymer aggregation is sustained by intermolecular amide N–H ··· O=C hydrogen bonds. The two pyridyl-groups show an *anti*-orientation and they are related by inversion at the centre of the molecule. As the six carbon atoms in the backbone are all in *anti*-conformation, the ligand extends its full length and the two pyridine nitrogen atoms are widely separated by 18.375(2) Å.

[Ag$_2$L$_3$OH][ClO$_4$]

Slow diffusion of an aqueous solution of $AgClO_4$ into 1 mol of L in ethanol produced crystals of [Ag$_2$L$_3$OH][ClO$_4$]·2.5H$_2$O. As shown by its X-ray crystal structure, the compound is

Table 1 Crystal data for the compounds

Compound	L	$[Ag_2L_3OH][ClO_4]\cdot 2.5H_2O$	$[AgL][ClO_4]$	$[AgL][NO_3]$	$[AgL][CF_3SO_3]$
Formula	$C_{18}H_{22}N_4O_2$	$C_{54}H_{72}Ag_2ClN_{12}O_{13.5}$	$C_{18}H_{22}AgClN_4O_6S$	$C_{18}H_{22}AgN_5O_5$	$C_{19}H_{22}AgF_3N_4O_5S$
Formula weight	326.40	1355.42	533.72	496.28	582.33
Crystal system	Monoclinic	Trigonal	Monoclinic	Triclinic	Triclinic
Space group	$P2(1)/c$	$P3(2)$	$C2/c$	$P\bar{1}$	$P\bar{1}$
a/Å	5.2078(8)	15.1300(2)	26.502(2)	5.0952(1)	9.1289(1)
b/Å	5.0943(8)	15.1300(2)	5.1431(4)	6.9931(2)	10.0509(2)
c/Å	30.930(5	22.1343(5)	44.366(3)	13.6355(4)	13.0946(2)
α/°	90	90	90	93.510(2)°	108.608(1)°
β/°	94.829(3)	90	94.348(2)	98.761(2)	107.677(1)
γ/°	90	120	90	95.219(2)	93.597(1)
V/Å^3	817.7(2)	4388.08(1)	6029.7(8)	476.80(2)	1067.82(3)
Z	2	3	12	1	2
μ/mm^{-1})	0.089	0.789	1.181	1.099	1.109
Final R indices[a]	$R1 = 0.0567$, $wR2 = 0.1113$	$R1 = 0.0608$, $wR\,2= 0.1359$	$R1 = 0.0481$, $wR2 = 0.1134$	$R1 = 0.0371$, $wR2 = 0.0868$	$R1 = 0.0339$, $wR2 = 0.0792$
R_{int}	0.0429	0.0212	0.0326	0.0206	0.0166
Final diff ρ_{max} (e Å^{-3})	0.207, −0.320	1.393, −0.998	1.133, −0.850	0.560, −0.592	0.502, −0.623
GOF[b]	0.915	1.041	1.003	1.078	1.135

[a] $R1 = (|F_o| - |F_c|)/(|F_o|)$; $wR2 = [w(F_o^2 - F_c^2)/w(F_o^4)]^{1/2}$. [b] Goodness of fit $= [(w(F_o^2 - F_c^2)^2/(n - p)]^{1/2}$. For all structures determined, the scan type is ω and the Mo-Kα wavelength is 0.71073 Å.

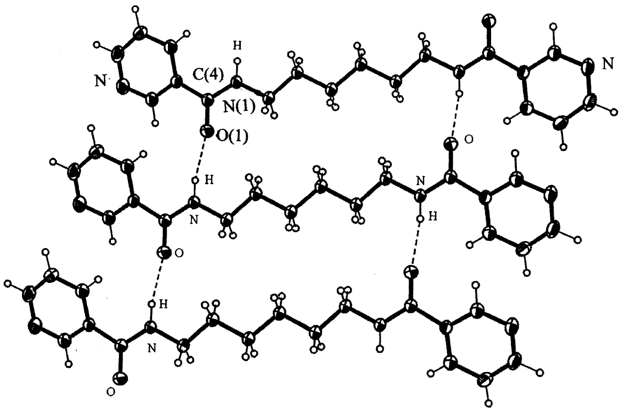

Fig. 1 ORTEP[21] plot of L (thermal ellipsoid 50%).

composed of interpenetrated hexagonal networks of Ag ions and ligands L extending along the *ab*-plane (Fig. 2a). Viewed along the *c*-axis, the network resembles a honeycomb, showing an infinite array of interconnected hexagons. Unlike most of the reported honeycomb networks, in which the hexagonal units are either planar,[15] or puckered (in either chair or boat conformation),[16] the net of $[Ag_2L_3OH][ClO_4]\cdot 2.5H_2O$ resembles an egg tray as the Ag ions occupying alternate nodal positions of the net are located in two different planes (Fig. 2a). These two sets of Ag ions, labeled as Ag(1) and Ag(2), are crystallographically independent. The Ag(1) ion is four-coordinate and in a distorted tetrahedral coordination including nitrogen atoms of three pyridyl groups and a hydroxide (Fig. 2b). The distance between the metal and oxygen, 2.514(7) Å, falls into the typical range of Ag–O bonds (≈2.3–2.6 Å)[17] (Table 3). Apparently the hydroxide ions came from the solvent water whose deprotonation could be facilitated by the Lewis acidic Ag ions. On the other hand, the Ag(2) ion is coordinated to three nitrogen atoms of the ligands L, showing a distorted trigonal planar geometry. The nodal silver ions in the two planes are connected by three ligands L, and accordingly the adjacent Ag(1) and Ag(2) are widely separated by 18.719(4) Å. The shortest distance between two Ag(1) ions (or two Ag(2) ions) is 15.130(4) Å. Each repeating $[Ag_6L_6OH_3][ClO_4]_3$ hexagon comprises three Ag(1) and three Ag(2) ions and possesses a crystallographic C_3-symmetry axis passing through its center and the equivalent Ag(1) or Ag(2) ions are related by C_3-rotation. Even though Ag(1) is four-coordinate, the hydroxide ion does not link to another Ag ion; hence in terms of connectivity, both Ag(1) and Ag(2) are the same and it would be appropriate to classify the present system as a (6,3)-net. The coordination of the long ligands L to the Ag ions gives rise to a tube-like structure surrounding the silver ions. Perchlorate ions are located in the cavity of the tubes. One of its oxygen atoms is 2.926(5) Å away from the Ag(2) ion and the other three O atoms are hydrogen bonded to amide N–H groups of the surrounding ligands L. There are 2.5 H_2O molecules per Ag ion in the crystal and they are possibly involved in hydrogen bonding interactions with the ligands L and the coordinated hydroxide ions (Fig. 2c and Table 4).

Table 2 Selected bond lengths (Å) and angles (°) in L

C(4)–O(1)	1.240(1)	O(1)–C(4)–N(1)	122.08(1)
C(4)–N(1)	1.341(2)	C(5)–C(4)–N(1)	116.99(1)

Table 3 Selected bond lengths (Å) and angles (°) in $[Ag_2L_3OH][ClO_4]\cdot 2.5H_2O$

Ag(1)–N(8)	2.260(6)	N(8)–Ag(1)–N(1)	110.9(2)
Ag(1)–N(1)	2.286(5)	N(8)–Ag(1)–N(5)	121.9(2)
Ag(1)–N(5)	2.289(7)	N(1)–Ag(1)–N(5)	119.9(2)
Ag(1)–O(7)	2.514(7)	N(8)–Ag(1)–O(7)	101.8(2)
Ag(2)–N(10)	2.277(7)	N(1)–Ag(1)–O(7)	104.5(2)
Ag(2)–N(11)	2.292(6)	N(5)–Ag(1)–O(7)	91.3(3)
Ag(2)–N(4)	2.292(5)	N(10)–Ag(2)–N(11)	118.9(2)
Ag(2)–O(11)	2.926(5)	N(10)–Ag(2)–N(4)	116.6(2)
Ag(2)–O(1S)	2.698(5)	N(11)–Ag(2)–N(4)	122.5(2)
C(6)–O(1)	1.219(8)	C(4)–C(6)–N(2)	117.1(6)
C(6)–N(2)	1.329(9)	O(1)–C(6)–N(2)	124.5(7)

Like many other hexagonal nets,[1f,15,16] the rugged nets in $[Ag_2L_3OH][ClO_4]\cdot 2.5H_2O$ show interpenetration. The large cavities in the tubes in one layer are partially filled with the tubes from its adjacent layers. Fig. 2b shows a pair of interlocked or catenated tubes. Interestingly, the interlocking only occurs between Ag(2)-containing and Ag(1)-containing tubes. Consequently, the Ag(1)- and Ag(2)-containing tubes within a layer are linked respectively with the Ag(2)- and Ag(1)-containing tubes of its two adjacent layers, as schematically represented in Fig. 2c.

$[AgL][ClO_4]$

X-Ray crystallographic analysis shows that the compound $[AgL][ClO_4]$ is a coordination polymer composed of ligands L and Ag(I) ions (Fig. 3a, for selected bond lengths and angles, see Table 5). Examining the bond parameters shows that there are two independent silver atoms which are slightly different in

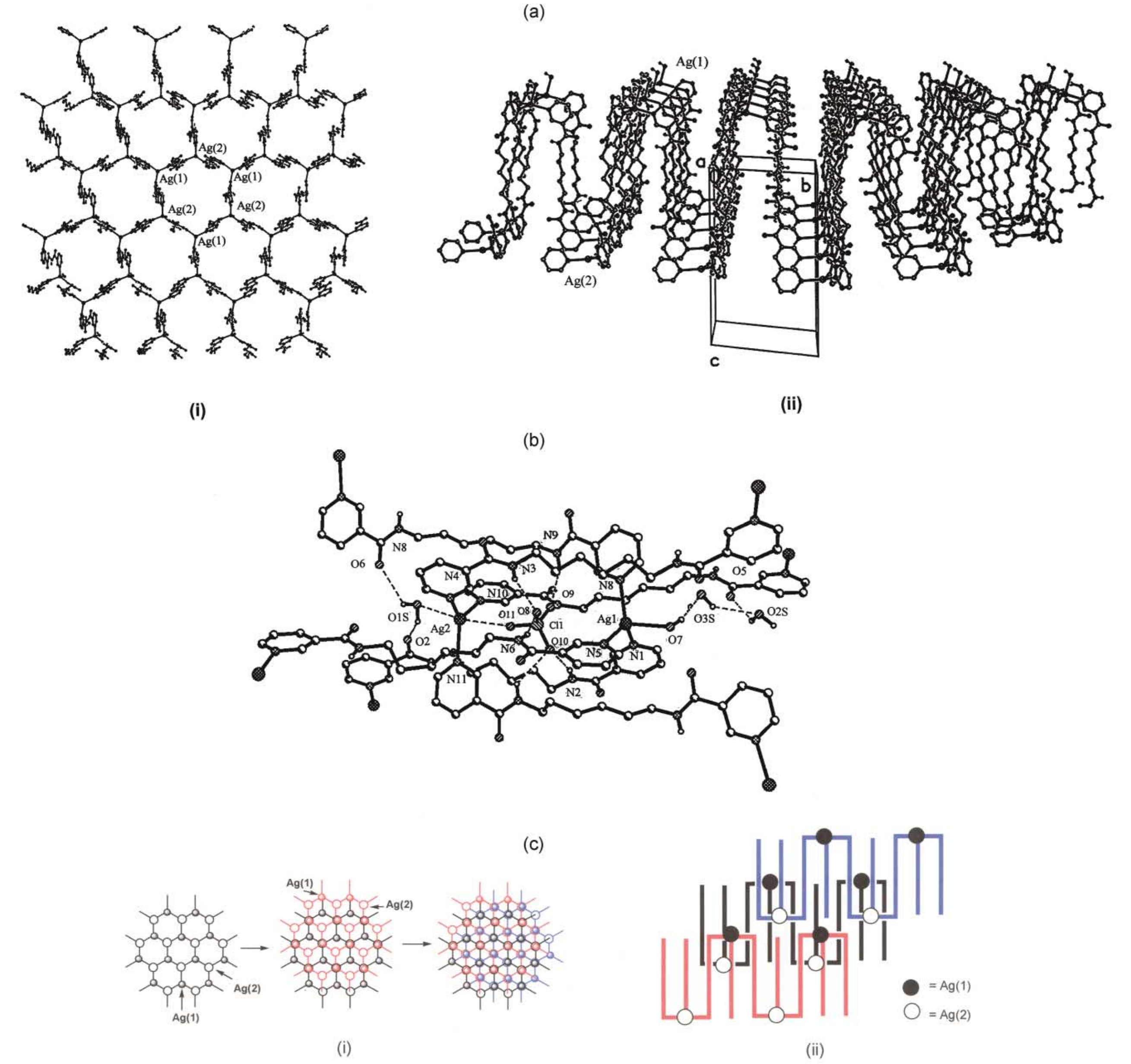

Fig. 2 (a) (i) Viewed along the *c*-axis, the X-ray crystal structure of a layer of $[Ag_2L_3OH][ClO_4]\cdot2.5H_2O$ shows a honeycomb-like structure. (ii) A cross section of a layer of $[Ag_2L_3OH][ClO_4]\cdot2.5H_2O$ along the *c*-axis showing the tube-like structures. (b) Diagram showing two interlocking molecular tubes and the position of the perchlorate ion and water molecules and possible hydrogen bonds. (c) (i) Schematic diagram showing the overlay of three adjacent layers in $[Ag_2L_3OH][ClO_4]\cdot2.5H_2O$. The overlapped circles represent positions where two tubes are interlocked. (ii) Diagram showing the interpenetration of the 2-D networks and interlocking of molecular tubes.

Table 4 Bond lengths and angles of hydrogen bonds in the compounds

Compound	D–H ··· A	D ··· A/Å	H ··· A/Å	D–H ··· A/°	Symmetry operator
L	N(1)–H(1) ··· O(1)	2.990	2.116	169.12	$x, y + 1, z$
$[Ag_2L_3OH][ClO_4]\cdot2.5H_2O$	O(7)–H(7A) ··· O(3S)	2.516	1.736	158.20	
	N(2)–H(2A) ··· O(10)	2.900	2.099	154.73	
	N(3)–H(3B) ··· O(8)	2.956	2.180	149.94	$x + y + 3, -x + 2, z + 1/3$
	N(6)–H(6a) ··· O(8)	2.973	2.149	160.14	
	N(7)–H(7B) ··· O(9)	3.119	2.488	130.75	$x + y + 2, -x + 2, z + 1/3$
	N(9)–H(9A) ··· O(9)	3.040	2.216	160.31	
	O(1S)–H(1SA) ··· O(2)	2.918	2.527	111.93	$x + y + 3, -x + 2, z + 1/3$
	O(1S)–H(1SB) ··· O(6)	2.770	2.310	110.77	$x + y + 4, -x + 2, z + 1/3$
	O(2S)–H(2SB) ··· O(5)	3.287	2.628	130.88	$y + 3, x - y, z + 2/3$
	O(3S)–H(3SA) ··· O(2S)	3.132	2.365	140.86	$x, y, z - 1$
$[AgL][ClO_4]$	N(2)–H(2A) ··· O(1)	3.052	2.229	157.56	$x, y - 1, z$
	N(3)–H(3A) ··· O(2)	3.002	2.150	166.47	$x, y + 1, z$
	N(6)–H(6A) ··· O(3)	3.000	2.177	157.54	$x, y + 1, z$
$[AgL][NO_3]$	N(2)–H(2A) ··· O(1)	2.970	2.166	155.58	$x - 1, y, z$
$[AgL][CF_3SO_3]$	N(2)–H(2) ··· O(2)	2.989	2.328	172.26	$-x + 1, -y + 1, -z + 1$
	N(4)–H(4) ··· O(1)	3.013	2.264	172.45	$-x + 1, -y, -z + 1$

Table 5 Selected bond lengths (Å) and angles (°) in [AgL][ClO$_4$]

Ag(1)–N(1)	2.173(4)	N(1A)–Ag(1)–N(1)	180.0(3)
Ag(2)–N(4)	2.191(4)	N(4)–Ag(2)–N(5)	173.15(1)
Ag(2)–N(5)	2.194(4)	N(2)–C(6)–O(1)	123.0(4)
C(6)–O(1)	1.225(5)	N(2)–C(6)–C(4)	116.6(4)
C(6)–N(2)	1.336(5)	N(3)–C(13)–O(2)	121.6(4)

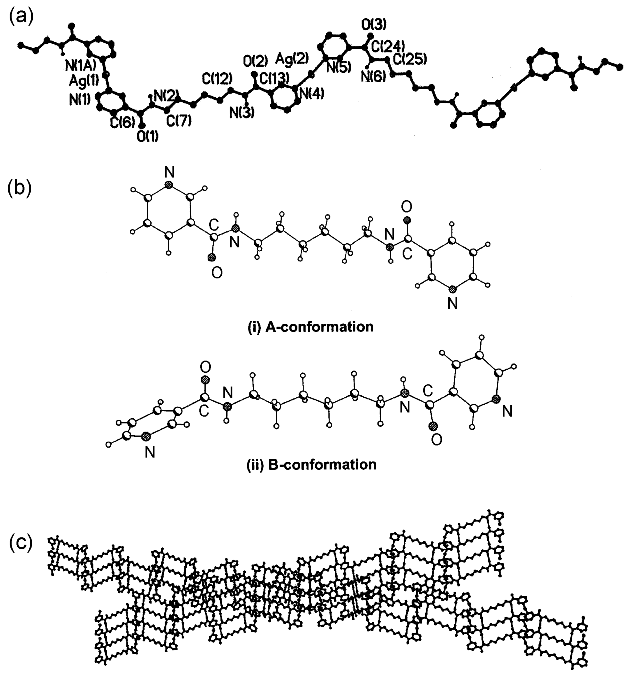

Fig. 3 (a) X-Ray crystal structure of [AgL][ClO$_4$]. (b) (i) The **A**-conformation of L in [AgL][ClO$_4$]. (ii) The **B**-conformation. (c) Diagram showing the 2-D rugged sheets arising from the self-assembly of the [AgL][ClO$_4$] coordination polymers.

Table 6 Selected bond lengths (Å) and angles (°) in [AgL][NO$_3$]

Ag(1)–N(1)	2.185(3)	N(1A)–Ag(1)–N(1)	180.00(1)
Ag(1)–O(2)	2.554(8)	N(1A)–Ag(1)–O(2)	96.51(2)
C(6)–O(1)	1.235(4)	N(1)–Ag(1)–O(2)	83.49(2)
C(6)–N(2)	1.330(4)	N(2)–C(6)–O(1)	122.3(3)

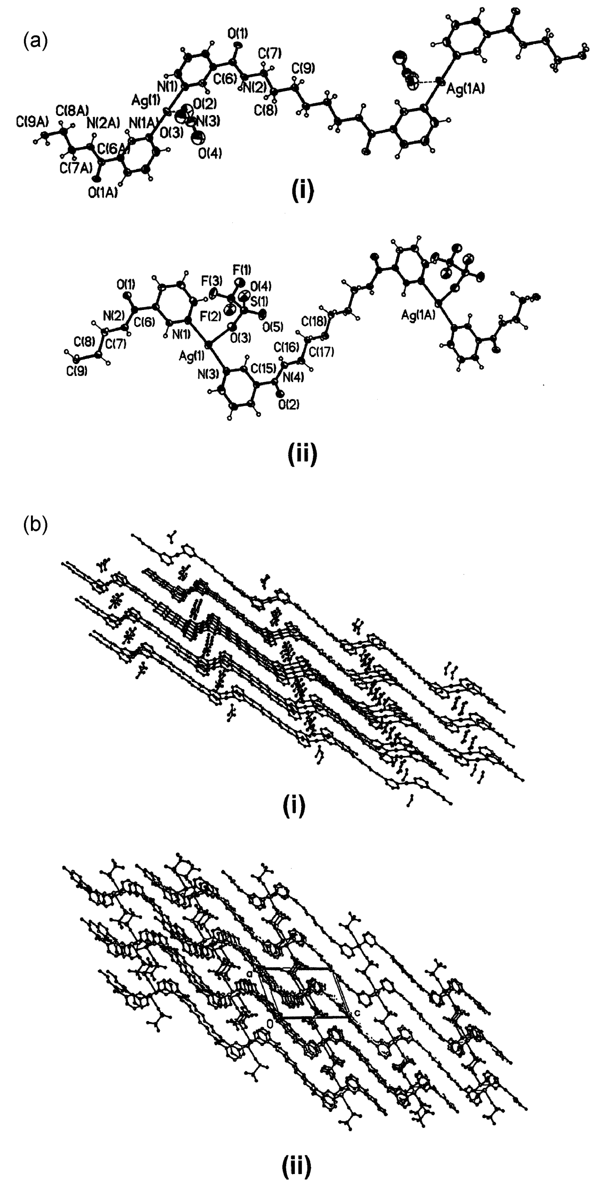

Fig. 4 (a) X-Ray crystal structures of (i) [AgL][NO$_3$] and (ii) [AgL][CF$_3$SO$_3$]. (b) Diagrams showing the solid-state stacking of the 2-D sheets of (i) [AgL][NO$_3$] and (ii) [AgL][CF$_3$SO$_3$].

their coordination geometry. One of the silver atoms, labeled as Ag(1), is coordinated to two nitrogen atoms of pyridyl groups in an ideal linear geometry, showing a N–Ag–N angle of 180.0(3)°. The metal ion lies on a centre of inversion. Whereas the other silver ions, labeled as Ag(2), show a slightly bent coordination geometry with a N(4)–Ag(2)–N(5) angle of 173.15(1)°. The Ag(1)–N bond length is slightly shorter than the one between N(4) and Ag(2). The Ag–N bond lengths lie within the normal range of 2.120–2.60 Å. The two pyridyl-rings that are connected by Ag(1) are coplanar while the two rings coordinated to Ag(2) show a small dihedral angle of 12°. In addition to these small differences in local coordination geometry, the ligands L coordinated to Ag(1) and Ag(2) adopt two different conformations **A** and **B** (Fig. 3b). The two conformations differ in the dihedral angle of the two pyridyl-rings: in the **A**-conformation, the two rings are nearly coplanar while in the **B**-conformation, the two rings show a dihedral angle of 83.3°. The two conformers are arranged periodically in a single strand of polymer in the sequence **ABBABBA**. The presence of **B**-conformation ligands gives the polymer a twisted conformation (Fig. 3c) which is different from the planar zigzag conformation of [AgL][NO$_3$] and [AgL][CF$_3$SO$_3$] (see later). The coordination polymers are linked together *via* complementary N–H ··· O=C hydrogen bonds between the adjacent chains, leading to 2-D undulating sheets (Fig. 3c). The parameters of the hydrogen bonds are given in Table 4. The shortest Ag–Ag distance between the two adjacent chains in a sheet is 5.143(2) Å. The stacking of sheets in [AgL][ClO$_4$] is staggered, forming a crisscross pattern as shown in Fig. 3c. The inter-sheet distance, defined as the shortest Ag–Ag distance between the two adjacent sheets, is 7.456(3) Å. The counter ions, ClO$_4^-$, are sandwiched between the adjacent sheets and associated with the silver atoms. The distance between the silver atom and the nearest Cl atom is 3.581(2) Å. The Ag–O distance is uncertain as the anion is disordered.

[AgL][NO$_3$] and [AgL][CF$_3$SO$_3$]

Crystals of [AgL][NO$_3$] were obtained by slow evaporation of an acetonitrile of the compound. However, crystals of [Agl][CF$_3$SO$_3$] could not be obtained by this method. We resorted to growing crystals of the compound by slow diffusion of a solution of the ligand into another solution of AgCF$_3$SO$_3$. Different combinations of solvents (*i.e.* H$_2$O/methanol, CH$_3$CN/H$_2$O) were tried and it was found that the solvent pair H$_2$O/MeOH gave the best result in terms of yield and quality of crystals. The X-ray crystal structures of [AgL][NO$_3$] and [AgL][CF$_3$SO$_3$] are highly similar as both compounds are composed of zigzag chains of AgL polymers (Fig. 4a and Tables 6

Table 7 Selected bond lengths (Å) and angles (°) in $[AgL][CF_3SO_3]$

Ag(1)–N(1)	2.167(2)	N(1)–Ag(1)–N(3)	172.64(9)
Ag(1)–N(3)	2.171(2)	N(1)–Ag(1)–O(3)	98.16(9)
Ag(1)–O(3)	2.584(2)	N(3)–Ag(1)–O(3)	89.15(8)
C(6)–O(1)	1.235(3)	N(2)–C(6)–O(1)	123.5(2)
C(6)–N(2)	1.330(3)	N(4)–C(15)–O(2)	123.4(2)

and 7). The Ag ions in both compounds show similar linear geometry and metal–ligand bond lengths ($[AgL][NO_3]$: N–Ag–N = 180.00(1)°, Ag–N = 2.185(3) Å; $[AgL][CF_3SO_3]$: N–Ag–N = 172.64(9)°, Ag–N = 2.167(2) and 2.171(2) Å). Unlike $[AgL][ClO_4]$, the ligands L in the present compounds are all in the **A**-conformation, giving the polymer chains a flat zigzag conformation. The NO_3^- and $CF_3SO_3^-$ ions in the compounds are closely associated with the Ag ion, showing Ag–O distances of 2.554(8) Å and 2.584(2) Å, respectively. The polymer chains of the compounds aggregate into 2-D corrugated sheets *via* complementary amide hydrogen bonds (Fig. 4b and Table 4). $[AgL][NO_3]$ (5.095(3) Å) and $[AgL][CF_3SO_3]$ (5.089(3) Å) show inter-chain Ag–Ag separations similar to the one observed in $[AgL][ClO_4]$ (5.143(2) Å). This suggests that the inter-chain separation in all of these compounds is governed mainly by the amide hydrogen bonds. The major difference between the two compounds is the inter-sheet distance. As shown in Fig. 4b, the corrugated sheets of $[AgL][NO_3]$ and $[AgL][CF_3SO_3]$ stack along the *b* axis and the NO_3^- and $CF_3SO_3^-$ ions are located between the slabs. In contrast to $[AgL][ClO_4]$, the stacking sheets of the compounds are in complete overlap. The inter-sheet Ag–Ag separations observed in the three silver compounds follow the order $[AgL][CF_3SO_3]$ (9.129(3) Å) > $[AgL][ClO_4]$ (7.456(3) Å) > $[AgL][NO_3]$ (6.993(3) Å). Reasonably, the trend parallels the size of the anions ($CF_3SO_3^-$ > ClO_4^- > NO_3^-) which occupy the space between the sheets.

Anion exchange

The anion exchange properties of the three coordination polymers [AgL][X] (X = ClO_4^-, NO_3^- and $CF_3SO_3^-$) were investigated using X-ray powder diffraction (XRPD), elemental analysis and infrared (IR) absorption spectroscopy. Our results show that immersion of the crystals of $[AgL][NO_3]$ in an aqueous solution of $LiClO_4$ for 12 h leads to complete replacement of NO_3^- with ClO_4^-. The IR spectrum of $[AgL][NO_3]$ shows an intense NO_3^- absorption band at 1384 cm^{-1} (Fig. 5a).[18] However, the absorption band does not appear in the IR spectrum of the solids obtained after the anion exchange. Instead, new and intense ClO_4^- bands show up at 1145–1089 cm^{-1}.[18] Other peaks of the spectrum remain virtually unchanged, suggesting the skeletal structure of the compound remains intact after the exchange process. The peaks of the XRPD pattern of the exchanged compound are slightly broadened, most probably due to the loss of crystallinity after the exchange. Nonetheless, the diffraction pattern closely resembles the experimental or simulated XRPD patterns of $[AgL][ClO_4]$ (Fig. 6a). Elemental analysis of the exchanged sample (Table 8) matches that of $[AgL][ClO_4]$. Analogous to $[AgL][NO_3]$, $CF_3SO_3^-$ ions in $[AgL][CF_3SO_3]$ can be replaced with ClO_4^- after suspending crystals of the compound in an aqueous solution $LiClO_4$ for 12 h. The IR spectrum shows the complete disappearance of the $CF_3SO_3^-$ band at 1261 cm^{-1} and the appearance of intense ClO_4^- bands at 1145–1089 cm^{-1} (Fig. 5b). The XRPD pattern is identical to that of $[AgL][ClO_4]$ (Fig. 6b). Elemental analysis (Table 8) also supports complete anion exchange.

While the exchange of $[AgL][NO_3]/[CF_3SO_3]$ with ClO_4^- is facile, the reverse process, $[AgL][ClO_4] + NO_3^-/CF_3SO_3^- \longrightarrow [AgL][NO_3]/[CF_3SO_3] + ClO_4^-$, was not observed even when crystals of $[AgL][ClO_4]$ were immersed in a concentrated solution (0.1 M) of $NaNO_3$ or $LiCF_3SO_3$ for two weeks. Similarly the inter-conversion $[AgL][NO_3] \leftrightarrow [AgL][CF_3SO_3]$ could not be achieved despite high salt concentration (0.1 M) and prolonged immersion (two weeks).

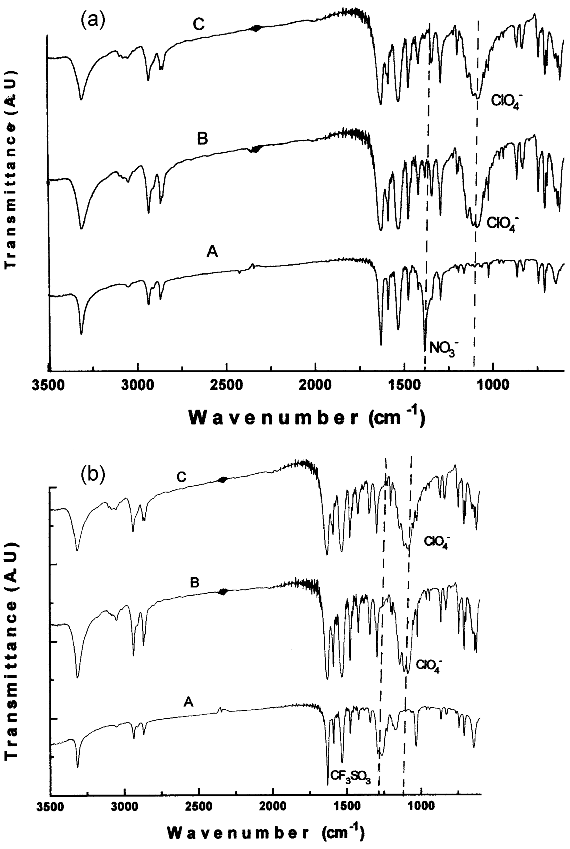

Fig. 5 (a) IR (KBr pellet) spectra of (A) $[AgL][NO_3]$ as prepared, (B) after exchange with $LiClO_4$, (C) $[AgL][ClO_4]$ as prepared. (b) IR (KBr pellet) spectra of (A) $[AgL][CF_3SO_3]$ as prepared, (B) after exchange with $LiClO_4$, (C) $[AgL][ClO_4]$ as prepared.

The anion exchange among the three coordination polymers is highly selective: only the conversion from $[AgL][NO_3]/[CF_3SO_3]$ to $[AgL][ClO_4]$ is possible. Selectivity of anion exchange has been observed in several coordination polymers[6,7] but its mechanism is not well understood. In some cases, anion exchange is accompanied by bond formation or dissociation[6] and a recent study[19] showed that the irreversibility of the exchange of $[Ag(bpp)][ClO_4]$ (bpp = 1,3-bis(4-pyridyl)propane) with PF_6^- is attributed to the formation of Ag–Ag interactions in $[Ag(bpp)][PF_6]$. However, it is unlikely to be the reason for the selective exchange observed in the present compounds as they show no obvious difference in bonding. Selectivity of anion exchange has been widely observed in anion resins[20] and was shown to be governed by the hydration energy (ΔG_h) of the anion, which is a function of its radius and charge. ΔG_h of the anions could play an important role in determining the selectivity. In addition, since the three compounds have different crystal structures and packing, inter-conversion of the compounds must require energy for the structural reorganization. The exchange of $[AgL][NO_3]$ with ClO_4^- is favored as ΔG_h of NO_3^- (−300 kJ mol^{-1}) is higher than that of ClO_4^- (−205 kJ mol^{-1}). Although ΔG_h of $CF_3SO_3^-$ ion is not known, it is expected to be smaller than those of ClO_4^- and NO_3^-. The difference in ΔG_h between NO_3^- and $CF_3SO_3^-$ may explain the fact that the exchange of $[AgL][CF_3SO_3]$ with NO_3^- is not feasible. Considering the hydration energy of the ions, it is anomalous that $CF_3SO_3^-$ cannot replace the anions in $[AgL][ClO_4]$ and $[AgL][NO_3]$. This suggests that there are factors other than ΔG_h in determining the anion exchange selectivity. The X-ray crystal structures of the compounds show that the inter-sheet distance in $[AgL][CF_3SO_3]$ (9.129(3) Å) is much longer than the ones in $[AgL][ClO_4]$ (7.456(3) Å) and

Table 8 Elemental analysis (EA) of [AgL][ClO_4] and the products obtained from the anion exchange

Elements	EA calculated for [AgL][ClO_4]	EA for a sample of [AgL][ClO_4]	EA for the product of the exchange reaction [AgL][NO_3] + $LiClO_4$ (aq)	EA for the product of the exchange reaction [AgL][CF_3SO_3] + $LiClO_4$ (aq)
C	40.46	40.57	40.37	40.60
H	4.12	4.09	4.14	4.05
N	10.57	10.63	10.57	10.48
Cl	6.64	6.60	6.52	6.40

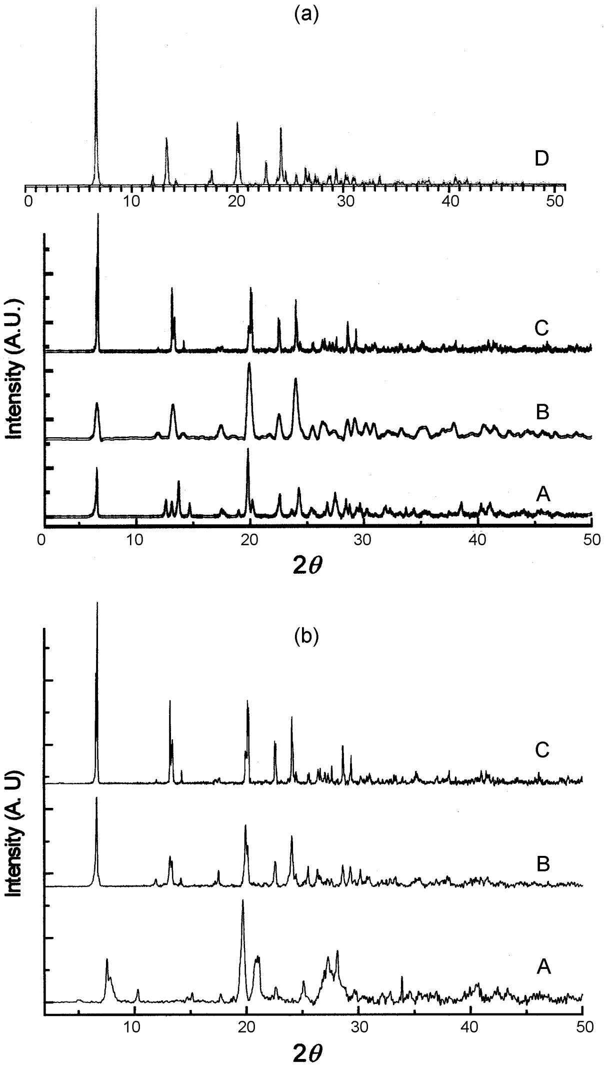

Fig. 6 (a) XRPD patterns of (A) [AgL][CF_3SO_3] as prepared, (B) solids obtained after immersing [AgL][CF_3SO_3] in an aqueous solution of $LiClO_4$ for 12 h, (C) [AgL][ClO_4] as prepared, (D) simulated for [AgL][ClO_4]. (b) XRPD patterns of (A) [AgL][NO_3] as prepared, (B) solids obtained after immersing [AgL][NO_3] in an aqueous solution of $LiClO_4$ for 12 h, (C) [AgL][ClO_4] as prepared.

[AgL][NO_3] (6.993(3) Å). Accordingly, considerable structural reorganization would be involved in the exchange and may render the process unfavorable. Another anomaly is that ClO_4^- is able to exchange with the anions in [AgL][CF_3SO_3] even though ΔG_h of the ions would suggest otherwise. A tentative explanation is that the close packed structure of [AgL][ClO_4] is preferable to the open structure of [AgL][CF_3SO_3].

Conclusions

In this study it was demonstrated that the ligand L can form coordination polymers of different topology. The compound [Ag_2L_3OH][ClO_4]·$2.5H_2O$ exhibits an unprecedented hexagonal interpenetrating net while [AgL][ClO_4] demonstrates an unusual co-existence of two ligand conformers in the same coordination polymer chain. In addition, the AgL polymers are able to zip up *via* inter-chain amide hydrogen bonds into 2-D undulating sheets. The anion exchange of the coordination polymer [AgL][X] (X = ClO_4^-, NO_3^- and $CF_3SO_3^-$) was shown to be selective and the anion exchange selectivity could be governed by the hydration energy of the anions and the energy required for structural reorganization.

Acknowledgements

J. H. K. Y. thanks the National University of Singapore for financial support. We are grateful to Ms Tan Geok Kheng for her assistance with the X-ray crystal structure determinations.

References

1 (*a*) B. F. Abrahams, B. F. Hoskins and R. Robson, *J. Am. Chem. Soc.*, 1991, **113**, 3603; (*b*) M. J. Zaworotko, *Chem. Commun*, 2001, 1; (*c*) O. M. Yaghi, H. Li, C. Davis, D. Richardson and T. L. Groy, *Acc. Chem. Res*, 1998, **31**, 474; (*d*) A. J. Blake, N. R. Champness, P. Hubberstey, W.-S. Li, M. A. Withersby and M. Schröder, *Coord. Chem. Rev.*, 1999, **183**, 117; (*e*) M. Munakata, L. P. Wu and T. Kuroda-Sowa, *Advances in Inorganic Chemistry*, Academic Press, New York, USA, ed. A. G. Sykes, 1999, vol. 46, p. 173; (*f*) S. R. Batten and R. Robson, *Angew. Chem., Int. Ed.*, 1998, **37**, 1460.

2 For linear chains see: (*a*) A. N. Khlobystov, A. J. Blake, N. R. Champness, D. A. Lemenovskii, A. G. Majouga, N. V. Zyk and M. Schröder, *Coord. Chem. Rev.*, 2001, **222**, 155; (*b*) R. H. Groeneman, L. R. MacGillivray and J. L. Atwood, *Inorg. Chem.*, 1999, **38**, 208; (*c*) S.-L. Zheng, M. L. Tong, X.-L. Yu and X.-M. Chen, *J. Chem. Soc., Dalton Trans.*, 2001, 586; (*d*) M. Maekawa, K. Sugimoto, T. Kuroda-Sowa, Y. Suenaga and M. Munakata, *J. Chem. Soc., Dalton Trans.*, 1999, 4357; (*e*) A. J. Blake, N. R. Champness, S. M. Howdle and P. B. Webb, *Inorg. Chem.*, 2000, **39**, 1035.

3 For 2-D networks see: (*a*) S. A. Barnett, A. J. Blake, N. R. Champness, J. E. B. Nicolson and C. Wilson, *J. Chem. Soc., Dalton Trans.*, 2001, 567; (*b*) M. L. Tong, S. L. Zheng and X.-M. Chen, *Chem. Eur. J.*, 2000, **6**, 3729; (*c*) I. Ino, L. P. Wu, M. Munakata, M. Maekawa, Y. Suenaga, T. Kuroda-Sowa and Y. Kitamori, *Inorg. Chem.*, 2000, **39**, 2146.

4 For 3-D networks see: (*a*) M. Eddaoudi, J. Kim, M. O'Keeffe and O. M. Yaghi, *J. Am. Chem. Soc.*, 2002, **124**, 376; (*b*) M. A. Withersby, A. J. Blake, N. R. Champness, P. A. Cooke, P. Hubberstey and M. Schröder, *J. Am. Chem. Soc.*, 2000, **122**, 4044; (*c*) T. Kuroda-Sowa, T. Horino, M. Yamamoto, M. Y. Ohno, H. Maekawa and M. Munakata, *Inorg. Chem.*, 1997, **36**, 6382; (*d*) B. Rather, B. Moulton, R. D. B. Walsh and M. Zaworotko, *Chem. Commun.*, 2002, 694.

5 (*a*) O. Kahn, *Acc. Chem. Res*, 2000, **33**, 647; (*b*) P. Long, E. B. Woodlock and X. Wang, *Inorg. Chem.*, 2000, **39**, 4174; (*c*) S. Noro, S. Kitazawa, M. Kondo and K. Seki, *Angew. Chem., Int. Ed.*, 2000, **39**, 2082; (*d*) J. Tao, J. X. Shi, M. L. Tong, X. X. Zhang and X.-M. Chen, *Inorg. Chem.*, 2001, **40**, 6328; (*e*) J. Zhang, R. G. Xiong, X. T. Chen, Z. L. Xue, S. M. Peng and X. Z. You, *Organometallics*, 2002, **21**, 235; (*f*) R. G. Xiong, X. Z. You, B. F. Abrahams, Z. L. Xue and C. M. Che, *Angew. Chem., Int. Ed.*, 2001, **40**, 4422.

6 (*a*) S.-I. Noro, R. Kitaura, M. Kondo, S. Kitagawa, T. Ishii, H. Matsuzaka and M. Yamashita, *J. Am. Chem. Soc.*, 2002, **124**, 2568; (*b*) K. S. Min and M. P. Suh, *J. Am. Chem. Soc.*, 2000, **122**, 6834; (*c*) O.-S. Jung, Y.-J. Kim, Y. A. Lee, H. K. Chae, H. G. Jang and J. Hong, *Inorg. Chem.*, 2001, **40**, 2105; (*d*) O. M. Yaghi and H. Li, *J. Am. Chem. Soc.*, 1995, **117**, 10401.

7 O-S. Jung, Y. J. Kim, Y. A. Lee, J. K. Park and H. K. Chae, *J. Am. Chem. Soc.*, 2000, **122**, 9921.

8 M. Eddaoudi, J. Kim, N. Rosi, D. Vodak, J. Wachter, M. O'Keefe and O. M. Yaghi, *Science*, 2002, **295**, 469.

9 S. Muthu, J. H. K. Yip and J. J. Vittal, *J. Chem. Soc., Dalton Trans.*, 2001, 3577.

10 (*a*) M. J. Plater, M. R. S. J. Foreman, T. Gelbrich and M. B. Hursthouse, *J. Chem. Soc., Dalton Trans.*, 2000, 1995; (*b*) M. J. Plater, M. R. S. J. Foreman, T. Gelbrich, S. J. Coles and M. B. Hursthouse, *J. Chem. Soc., Dalton Trans.*, 2000, 3065; (*c*) E. Lee, J. Kim, J. Heo, D. Whang and K. Kim, *Angew. Chem., Int. Ed.*, 2001, **40**, 399.

11 *SMART & SAINT Software Reference Manuals, Version 4.0*, Siemens Energy & Automation, Inc., Analytical Instrumentation, Madison, WI, 1996.

12 G. M. Sheldrick, SADABS, software for empirical absorption correction, University of Göttingen, Göttingen, Germany, 1996.

13 *SHELXTL Reference Manual, Version 5.03*, Siemens Energy & Automation, Inc., Analytical Instrumentation, Madison, WI, 1996.

14 R. Taylor and O. Kennard, *Acc. Chem. Res.*, 1984, **14**, 320.

15 (*a*) G. Saito, H. Yamochi, T. Nakamura, T. Komatsu, N. Matsukawa, T. Inoue, H. Ito, T. Ishiguro, M. Kusunoki, K. Sakaguchi and T. Mori, *Synth. Met.*, 1993, **55–57**, 2883; (*b*) L. R. MacGillivary, S. Subramanian and M. Zaworotko, *J. Chem. Soc., Chem. Commun.*, 1994, 1325; (*c*) J. Konnert and D. Britton, *Inorg. Chem.*, 1966, **5**, 1193; (*d*) S. R. Batten, B. F. Hoskins and R. Robson, *New. J. Chem.*, 1998, **22**, 173.

16 (*a*) M.-C. Brandys and R. J. Puddephatt, *J. Am. Chem. Soc.*, 2002, **124**, 3946; (*b*) D. Whang and K. Kim, *J. Am. Chem. Soc*, 1997, **119**, 451; (*c*) M. Hong, W. Su, R. Cao, M. Fujita and J. Lu, *Chem. Eur. J.*, 2000, **6**, 427–431; (*d*) S. L. Zheng, M. L. Tong, R.-W. Fu, X.-M. Chen and S.-W. Ng, *Inorg. Chem.*, 2001, **40**, 352–3569; (*e*) M. Munakata, L. P. Wu, T. Kuroda-Sowa, M. Maekawa, K. Moriwaki and S. Kitagawa, *Inorg. Chem.*, 1997, **36**, 5416–5418; (*f*) L. Carlucci, G. Ciani, D. W. von Gudenberg, D. M. Proserpio and A. Sironi, *Chem. Commun.*, 1997, 631.

17 F. H. Allen and O. Kennar, *Chem. Des. Automat. News*, 1993, **8**, 31.

18 K. Nakamoto, *Infrared and Raman spectra of inorganic and coordination compounds*, John Wiley & Sons, Inc., New York, 1997.

19 L. Pan, B. Woodlock, X. Wang, K.-C. Lam and A. L. Rheingold, *Chem. Commun.*, 2001, 1762.

20 B. A. Moyer and P. V. Bonnesen, in *Supramolecular Chemistry of Anions*, eds. A. Bianchi, K. Bowman-James and E. García-España, John Wiley and Sons, Inc., New York, 1997, pp. 34–40.

21 C. K. Johnson, ORTEP, Report ORNL-5138, Oak Ridge National Laboratory, Oak Ridge, TN, 1976.